Supporting Information

Methodological Improvement in Pulsed Laser-Induced Size Reduction of Aqueous Colloidal Gold Nanoparticles by Applying High Pressure

Daniel Werner, Tomoyuki Ueki, and Shuichi Hashimoto*

Department of Ecosystem Engineering, The University of Tokushima, Tokushima 770-8506, Japan.

*Corresponding author. E-mail: hashi@eco.tokushima-u.ac.jp

Contents:

1. Particle images (TEM micrographs) and corresponding size distributions of Au NPs employed in this study

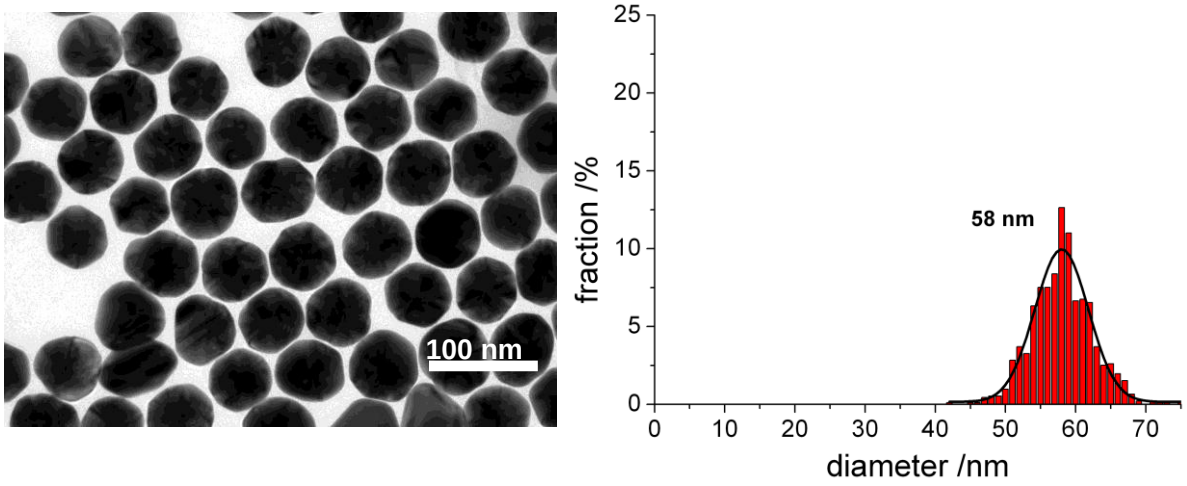

Figure S1. TEM picture and corresponding histogram of size distribution for aqueous Au NPs from British Biocell International (EMGC60). For the construction of a histogram, 918 particles were measured. The NPs show faceted shapes typical of chemical preparation.

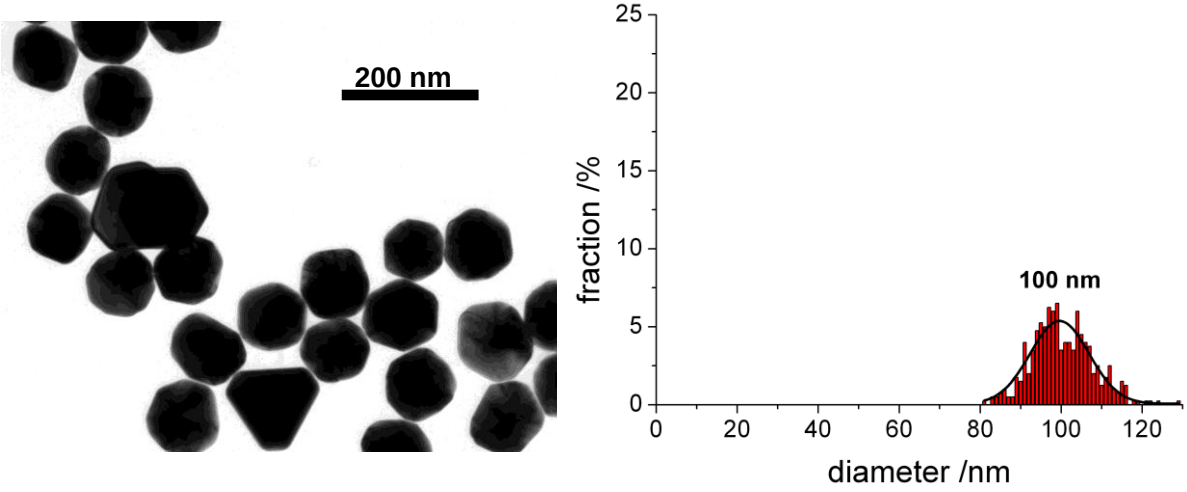

Figure S2. TEM picture and corresponding size distribution of aqueous Au NPs from British Biocell International (EMGC100). The particle number of 400 was measured.

2. Particle images (TEM micrographs) and corresponding histograms for original 58-nm gold NPs obtained after laser irradiation at 0.1 MPa

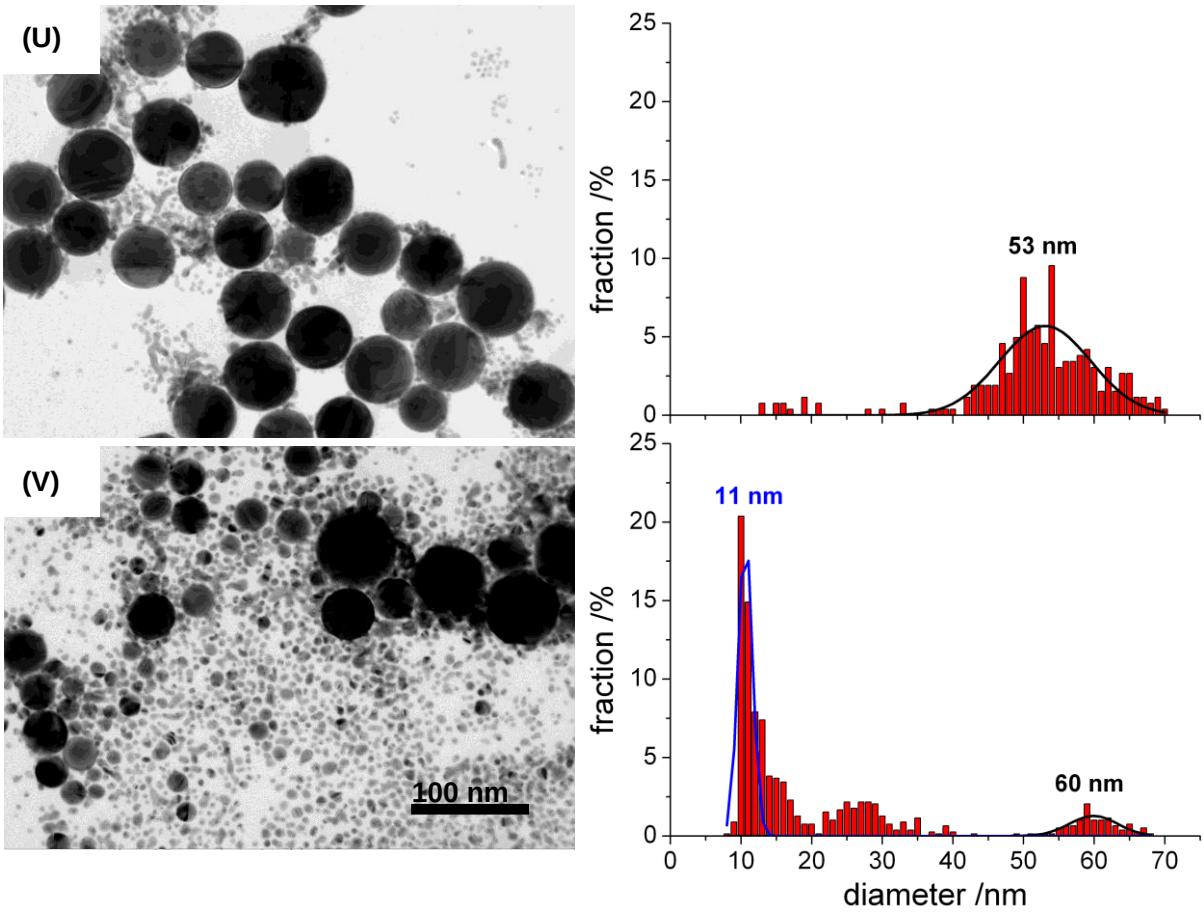

Figure S3. TEM images and corresponding size distributions of initial 58 nm diameter Au NPs irradiated with 18,000 pulses at an excitation wavelength of 532 nm under the pressure of 0.1 MPa. The laser energy densities are (U) 34.7 mJ·cm^{-2} and (V) 59.2 mJ·cm^{-2}. In Figure S3, 262 particles (U) and 785 particles (V) were measured. The notations (U) and (V) correspond to the data points given in Fig. 2. The 100-nm scale is applicable to both images.

3. Histograms for original 58-nm gold NPs obtained after laser irradiation at 150 MPa

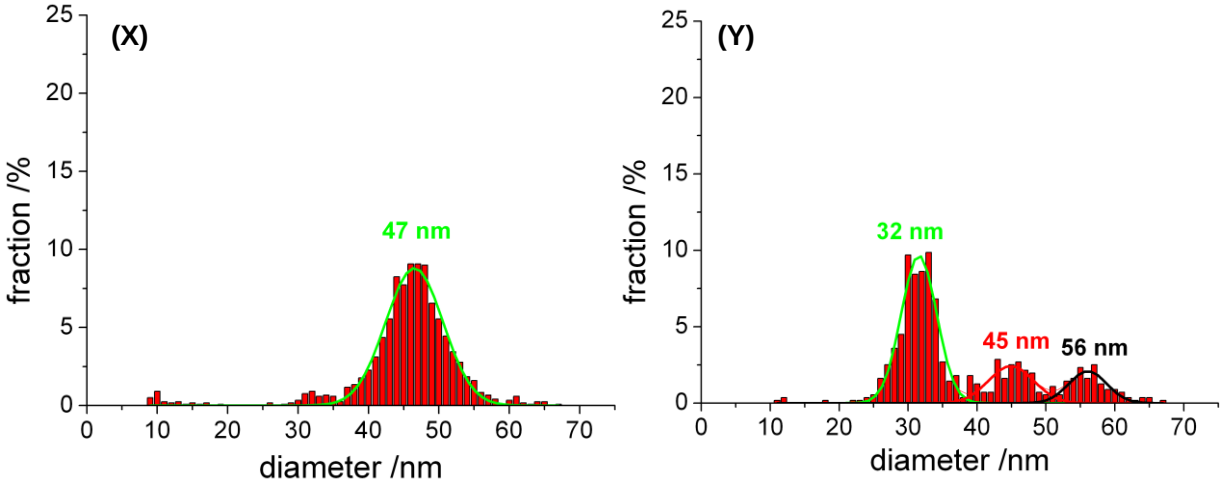

Figure S4. Histograms representing the size distribution of original 58-nm Au NPs after 30-min of pulsed-laser-irradiation at 10 Hz. The pressure was 150 MPa. The laser intensities are 99.7 mJ cm^{-2} (X) and 115.5 mJ cm^{-2} (Y). For the construction of histograms, 1190 particles (X) and 557 particles (Y) were measured. The notations (X) and (Y) correspond to the data points in Figure 2.

4. Particle images (TEM micrographs) and corresponding size distribution of initial 58-nm Au NPs after 355-nm pulsed laser excitation at 60 MPa

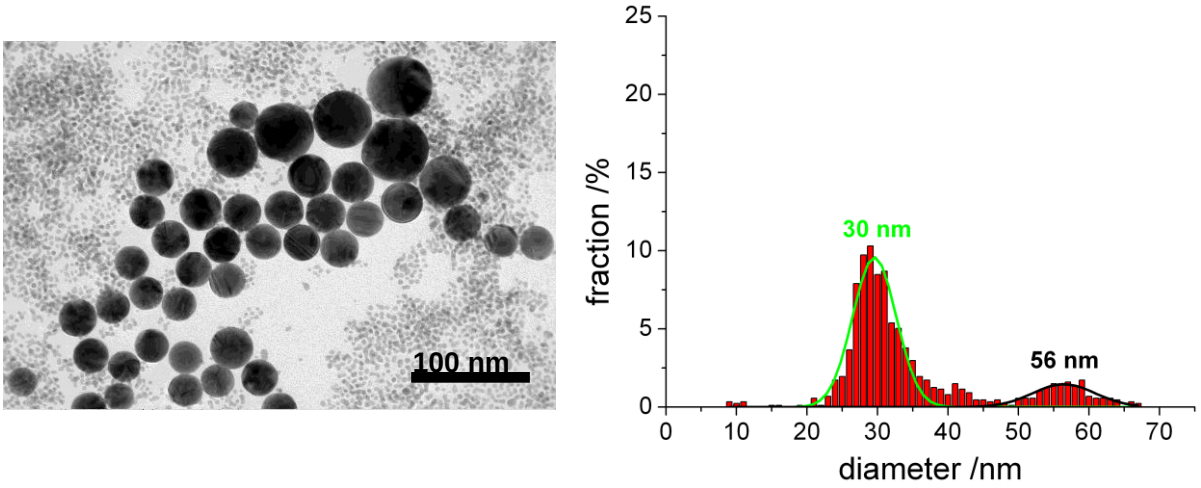

Figure S5. Particle image (TEM photograph) and corresponding size distribution of original 58-nm Au NPs after 18,000 shots (30 min at 10 Hz) on excitation with 355 nm laser light (60 MPa, 70.4 mJ cm^{-2}). For the construction of a histogram, 874 particles were measured.

The effects of excitation wavelength were investigated to see if the interband excitation at 355 nm gives results different from that of intraband excitation of conduction electrons (or LSPR band excitation) at 532 nm. No difference was observed. A TEM photograph together with the corresponding size distribution for the excitation of 58-nm particles at 60 MPa is given in Supporting Information Figure S5.

5. Supplementary figures of pulsed-laser-induced size reduction of aqueous 100-nm Au NPs

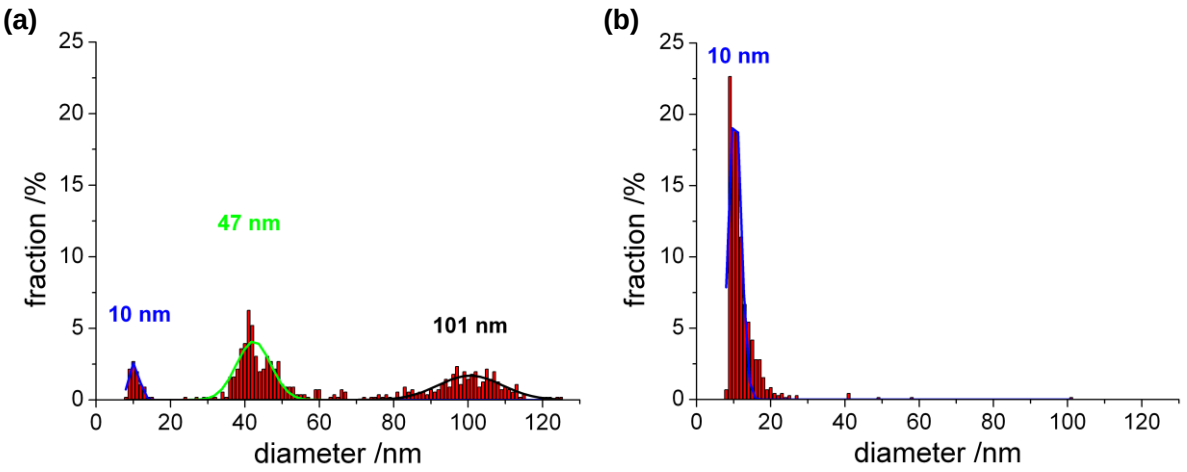

Figure S6. Size distributions of 100-nm diameter Au NPs obtained after irradiation of 18,000 pulses (30min, 10 Hz) at (a) 60 MPa, 78 mJ cm^{-2} and (b) 0.1 MPa, 59.9 mJ cm^{-2}. The excitation laser wavelength was 532 nm. For the construction of histograms, particles sizes were measured for 559 (a) and 720 (b) particles.

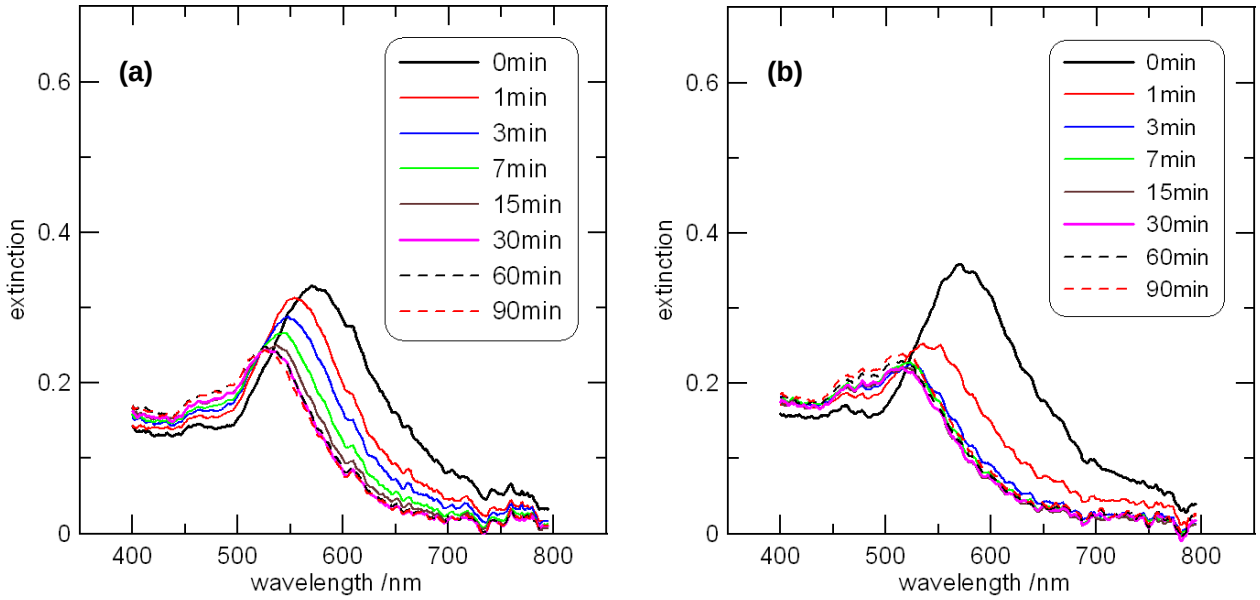

Figure S7. *In situ* spectra of original 100-nm diameter Au NPs in aqueous solution obtained during the pulsed-laser-irradiation at (a) 50.5 mJ cm^{-2} and (b) 75.8 mJ cm^{-2}. The excitation wavelength was 532 nm and a pressure applied was 60 MPa. A distinct reduction and blue-shift in the LSPR band indicate the size reduction.

6. Pressure-dependent boiling point of bulk gold

The Clausius–Clapeyron equation for the liquid–vapor equilibrium was used to determine the boiling point of bulk gold at various external pressures.

$$\ln\left(\frac{p}{p_{atm}}\right) = \frac{\Delta H_{evap}}{R} \cdot \left(\frac{1}{T_{atm}} - \frac{1}{T_{bp}}\right) \qquad (1)$$

Here R and ΔH_{evap} are the gas constant (8.314 $J \cdot mol^{-1} \cdot K^{-1}$) and the molar evaporation enthalpy of gold (334.4 $kJ \cdot mol^{-1}$), respectively. The boiling point T_{atm} at the atmospheric pressure (p_{atm} = 0.1 MPa) is 3129 K for bulk gold. By incorporating these values into equation 1, pressure-dependent boiling point T_{bp} was calculated. Figure S8 shows the boiling point of bulk gold as a function of pressure up to 400 MPa.

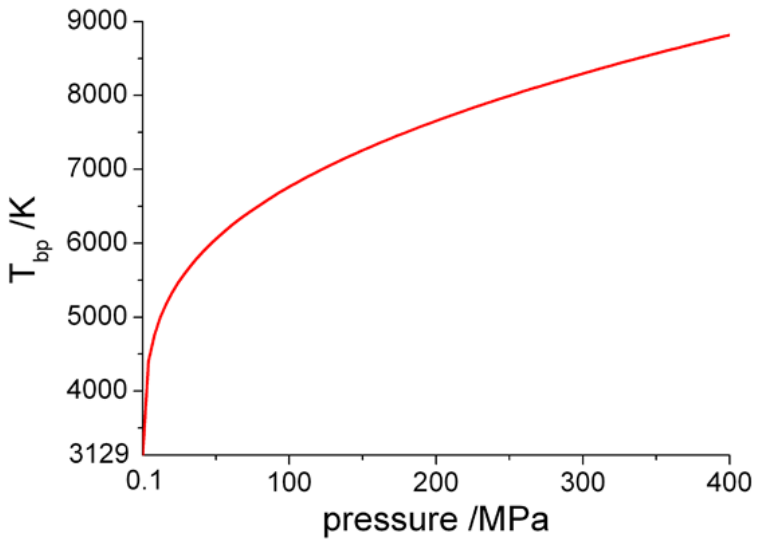

Figure S8. Pressure-dependent boiling point of bulk gold calculated by applying the Clausius–Clapeyron equation.

7. Pressure-dependent optical properties of Au NPs and water

In contrast to the increased values of the thermophysical properties, which act to suppress the temperature increase of Au NPs, both the scattering and the absorption efficiencies increase with increasing pressure. This is because the refractive index of water is sensitive to both the external pressure and temperature.[1] With increasing external pressure, the refractive index increases and brings about an increased extinction (absorption and scattering) of the aqueous colloidal Au NPs.[2] This effect has been pointed out previously.[3,4] Experimental extinction spectral changes on application of 60 MPa are shown in Figure S9 together with the calculated spectra based on the Mie theory. The absorption cross-section of Au NPs of diameter 55 nm as a function of the pressure-dependent refractive index of water is given in Figure S10, and curves of the pressure- and temperature-dependent refractive index of water are given in Figure S11. Inspection of Figures S9 and S10 reveals that this effect is rather small for the absorption of the Au NPs at room temperature, but significant differences in the refractive index, depending on pressure, occur at increased water temperatures (Figure S11). Higher pressures lead to smaller drops in the refractive index curve with increasing temperature. This causes the rises in the absorption efficiency of the Au NPs dispersed in water during the pulsed laser heating process.

[References]

1. Schiebener, P.; Straub, J.; Sengers, J. M. H. L.; Gallagher, J. S. *J. Phys. Chem. Ref. Data* **1990**, 19, 677-717.
2. Bohren, C. F.; Huffman, D. R. *Absorption and Scattering of Light by Small Particles*; Wiley: New York, **1983**.
3. Coffer, J. L.; Shapley, J. R.; Drickamer, H. G. *J. Am. Chem. Soc.* **1990**, 112, 3736-3742.
4. Christofilos, D.; Assimopoulos, S.; Fatti, N. D.; Voisin, C.; Vallèe, F.; Kourouklis, G. A.; Ves, S. *High Pressure Research* **2003**, 23, 23-27.

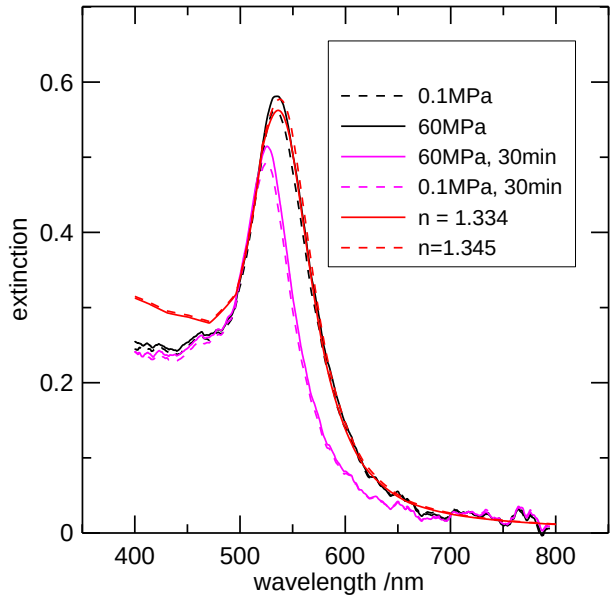

Figure S9. Extinction spectra of aqueous 58-nm Au NPs measured at the atmospheric pressure (black dashed line) and 60 MPa (black solid line) together with the spectra obtained after 30 min of pulsed-laser-irradiation at 532 nm (49.1 mJ·cm^{-2}) before (solid magenta line) and after pressure (dashed magenta line) release. Spectral fittings by the application of the Mie theory with the refractive indices of n = 1.334 (0.1 MPa) and n = 1.345 (60 MPa) were also included.

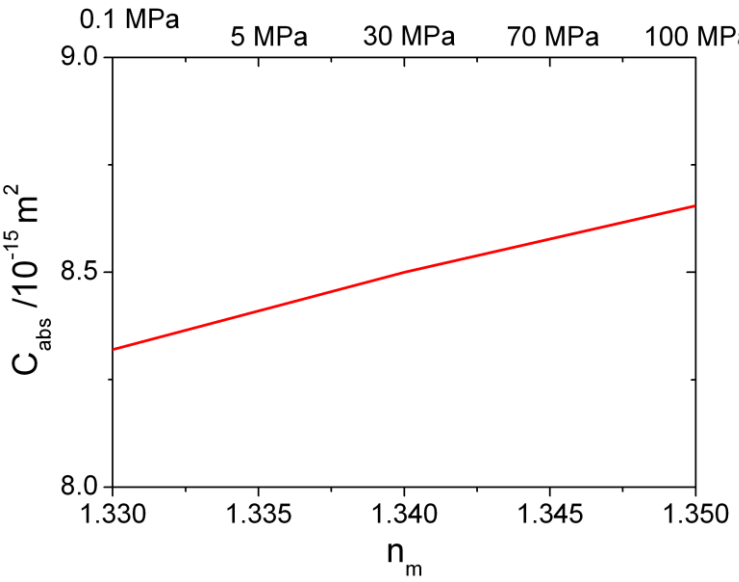

Figure S10. Absorption cross section C_{abs} of a 55 nm Au sphere submerged in water at different external pressures and thus medium refractive indices. The excitation wavelength was 532 nm. Only slight changes in C_{abs} can be expected at pressures between 0.1 MPa and 100 MPa.

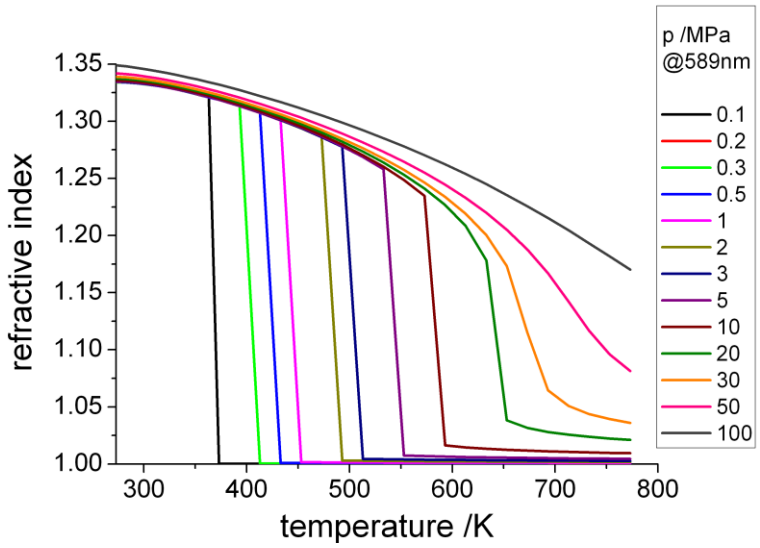

Figure S11. Refractive index of water at 589 nm versus temperature curves dependent on pressure. The curves were produced from the tabulated data in ref. 42. The refractive indices fall rapidly with increasing temperature. However, the slope of this fall is lower with increasing pressure.